Precursor Oxidation State Control of Film Stoichiometry in the Metal−Organic Chemical Vapor Deposition of Tin Oxide Thin Films

Seigi Suh and David M. Hoffman*

Department of Chemistry, University of Houston, Houston, Texas 77204

Lauren M. Atagi and David C. Smith

Los Alamos National Laboratory, Los Alamos, New Mexico 87545

Jia-Rui Liu and Wei-Kan Chu

Texas Center for Superconductivity, University of Houston, Houston, Texas 77204

Received August 8, 1996. Revised Manuscript Received December 18, 1996[⊗]

A new tin(IV) hexafluoroisopropoxide complex and a related tin(II) compound were used as low-pressure chemical vapor deposition precursors to tin oxide thin films. The films were characterized by backscattering and elastic recoil spectrometries, Auger and UV−vis spectroscopies, and nuclear reaction analysis. $Sn(OCH(CF_3)_2)_4(HNMe_2)_2$, a volatile solid (subl 70−75 °C at 0.06 Torr), was synthesized in high yield by reacting $Sn(NMe_2)_4$ with $(CF_3)_2$-CHOH. A crystal structure determination shows that it has an octahedral structure with *trans*-amine ligands. Low-pressure chemical vapor deposition using $Sn(OCH(CF_3)_2)_4$-$(HNMe_2)_2$ and air as precursors gave fluorine-doped tin oxide films (O/Sn = 1.8−2.4; F/Sn = 0.005−0.026) at substrate temperatures of 200−450 °C. The films are highly transparent in the visible region (>85%) and have resistivities as low as 2.1×10^{-3} Ω cm. In contrast to the results obtained for the tin(IV) precursor, the tin(II) compound $Sn(OCH(CF_3)_2)_2$-$(HNMe_2)$ in combination with air or water vapor gave nonconductive transparent films at substrate temperatures of 180−250 °C having composition $SnO_{0.9-1.3}F_{0.1-0.4}$. These film stoichiometries suggest that hydrolysis was the primary film-forming reaction and that the tin was not oxidized in the deposition process.

Doped tin oxide films are transparent conductors that are used as electrodes in thin-film solar cells, liquid-crystal displays, electrochromic devices and other optoelectronic device applications.[1] Fluorine is the preferred dopant because it gives films with the highest transparency and conductivity. [1,2]

Deposition methods for SnO_2 films include spray pyrolysis,[3] sputtering,[4,5] and chemical vapor deposition.[2,6−20] Chemical vapor deposition (CVD) is the method of choice because it allows for good control of film properties and gives high growth rates using simple, inexpensive equipment. One of the most successful CVD fluorine-doped tin oxide deposition systems uses $SnMe_4$ and oxygen precursors in combination with the fluorine dopant $BrCF_3$ at deposition temperatures >440 °C.[2,12,13] Other reported tin oxide CVD precursors include $SnCl_4$,[10,11,15−18] $Sn(n\text{-}Bu)_2(OAc)_2$,[6,7] $Sn(acac)_2$,[16] $Sn(OAc)_2$,[14] $Sn(NMe_2)_4$,[19] and $Sn(O\text{-}t\text{-}Bu)_4$.[20]

Recently, a new CVD precursor system for fluorine-doped SnO_2 was introduced, $Sn(O_2CCF_3)_2$ and air, where the precursor ligand serves as the fluorine source.[14] By using this system, films grown at 350 and 450 °C had F/Sn ratios of 0.026 and 0.028, respectively, and a sample grown at 400 °C had a resistivity of 6×10^{-4} Ω cm, which is comparable to the best CVD films. Motivated by this result, we became interested in synthesizing other potential fluorine-doped tin oxide precursors

[⊗] Abstract published in *Advance ACS Abstracts,* February 1, 1997.

(1) Chopra, K. L.; Major, S.; Pandya, D. K. *Thin Solid Films* **1983**, *102*, 1.
(2) Proscia, J.; Gordon, R. G. *Thin Solid Films* **1992**, *214*, 175.
(3) Yagi, I.; Ikeda, E.; Kuniya, Y. *J. Mater. Res.* **1994**, *9*, 663 and references therein.
(4) Semancik, S.; Cavicchi, R. E. *Thin Solid Films* **1991**, *206*, 81.
(5) Leja, E.; Pisarkiewicz, T.; Kolodziej, A. *Thin Solid Films* **1980**, *67*, 45.
(6) Kane, J.; Schweizer, H.; Kern, W. *J. Electrochem. Soc.* **1975**, *122*, 1144.
(7) Kane, J.; Schweizer, H.; Kern, W. *J. Electrochem. Soc.* **1976**, *123*, 270.
(8) Hsu, Y.-S.; Ghandhi, S. K. *J. Electrochem. Soc.* **1979**, *126*, 1434.
(9) Chow, T. P.; Ghezzo, M.; Baliga, B. J. *J. Electrochem. Soc.* **1982**, *129*, 1040.
(10) Saxena, A. K.; Thangaraj, R.; Singh, S. P.; Agnihotri O. P. *Thin Solid Films* **1985**, *131*, 121.
(11) Mizuhashi, M.; Gotoh, Y.; Adachi, K. *Jpn. J. Appl. Phys.* **1988**, *27*, 2053.
(12) Gordon, R. G.; Proscia, J.; Ellis, Jr., F. B.; Delahoy, A. E. *Solar Energy Mater.* **1989**, *18*, 263.
(13) Borman, C. G.; Gordon, R. G. *J. Electrochem. Soc.* **1989**, *136*, 3820.
(14) Maruyama, T.; Tabata, K. *J. Appl. Phys.* **1990**, *68*, 4282.
(15) Sanon, G.; Rup, R.; Mansingh, A. *Thin Solid Films* **1990**, *190*, 287.
(16) Maruyama, T.; Ikuta, Y. *Sol. Energy Mater. Sol. Cells* **1992**, *28*, 209.
(17) Banerjee, R.; De, A.; Ray, S.; Barua, A. K.; Reddy, S. R.; *J. Phys. D: Appl. Phys.* **1993**, *26*, 2144.
(18) Kim, K. H.; Lee, S. W.; Shin, D. W.; Park, C. G. *J. Am. Ceram. Soc.* **1994**, *77*, 915.
(19) Atagi, L. M.; Hoffman, D. M.; Liu, J.-R.; Zheng, Z.; Chu, W.-K.; Rubiano, R. R.; Springer, R. W.; Smith, D. C. *Chem. Mater.* **1994**, *6*, 360.
(20) Houlton, D. J.; Jones, A. C.; Haycock, P. W.; Williams, E. W.; Bull, J.; Critchlow, G. W. *Chem. Vap. Deposition* **1995**, *1*, 26.

S0897-4756(96)00423-1 CCC: $14.00 © 1997 American Chemical Society

having fluorinated ligands. We chose as a ligand hexafluoroisopropoxide, $OCH(CF_3)_2$, because alkoxide complexes are known to be viable oxide film precursors[21−25] and metal hexafluoroisopropoxide complexes are reported to decompose to metal fluorides under certain conditions.[26] In this paper we describe the synthesis and structural characterization of $Sn(OCH(CF_3)_2)_4(HNMe_2)_2$ and low-pressure CVD studies using it and the previously reported complex $Sn(OCH(CF_3)_2)_2(HNMe_2)$ as thin-film precursors.

Experimental Section

Synthesis. General Procedures. All manipulations were carried out in a glovebox and by using standard Schlenk techniques. $(CF_3)_2CHOH$ was purchased from Aldrich and was degassed before use. Ether and hexanes were distilled from Na/benzophenone and then stored in the drybox over 4 Å molecular sieves until they were needed. $Sn(NMe_2)_4$[27] and $Sn(OCH(CF_3)_2)_2(HNMe_2)$[28] were prepared by the literature methods, and their purities were checked by NMR (>98% pure). Infrared spectra were obtained using a Mattson Galaxy 5000 FTIR, and NMR spectra were collected on a GE 300-MHz instrument. Elemental analyses were performed by Oneida Research Services, Whitesboro, NY.

$Sn(OCH(CF_3)_2)_4(HNMe_2)_2$. A solution of $(CF_3)_2CHOH$ (2.83 g, 16.8 mmol) in ether (7 mL) was added dropwise to a cold solution (−78 °C) of $Sn(NMe_2)_4$ (1.24 g, 4.20 mmol) in ether (20 mL). The reaction mixture was allowed to warm to room temperature slowly after the addition was completed. After stirring the solution at room temperature for 1 h, the mixture was stripped to dryness in vacuo to give a white solid. The solid was dissolved in ether and the solution was slowly cooled to −35 °C to give the product as colorless crystals (yield 3.28 g, 89%). The compound can be vacuum sublimed as a white powder (70−75 °C, 0.06 mmHg). Anal. Calcd for $C_{16}H_{18}N_2O_4F_{24}Sn$: C, 21.91; H, 2.07; N 3.19. Found: C, 21.88; H, 1.82; N, 2.89.

^1H NMR (C_6D_6) δ 4.73 (br s, 4, $OCH(CF_3)_2$), 3.17 (br s, 2, $HNMe_2$), 1.94 (s, 12, $HNMe_2$). $^{13}C\{^1H\}$ NMR (C_6D_6) 123.2 (q, 8, $^1J_{CF}$ = 284 Hz, $OCH(CF_3)_2$), 73 (septet, 4, $^2J_{CF}$ = 32 Hz, $OCH(CF_3)_2$), 39.4 (s, 2, $HNMe_2$). IR (Nujol, CsI, cm^{-1}) 3321 m, 1287 s, 1258 s, 1184 s, 1147 s, 1067 s, 1018 m, 887 s, 856 s, 748 s, 687 s, 525 m.

X-ray Structure Determination. Crystal data for $Sn(OCH(CF_3)_2)_4(HNMe_2)_2$ are presented in Table 1, and final atomic coordinates in Table 2. The crystals were handled under mineral oil because of their air sensitivity. A colorless fragment was cut from a large prismatic block and mounted in a random orientation on a Nicolet R3m/V automatic diffractometer equipped with a low-temperature device. The Laue symmetry was determined to be 2/*m*, and from the systematic absences the space group was shown unambiguously to be $P2_1/n$. Intensities were measured using the Ω-scan technique. Two standard reflections were monitored after every 2 h or every 100 data collected, and these showed no significant change. During data reduction Lorentz and polarization corrections were applied, but an absorption correction was not found to be necessary.

The structure was solved using the SHELXTL Patterson interpretation program which revealed the position of the Sn atom. The remaining atoms were located in subsequent difference Fourier syntheses. The usual sequence of isotropic and anisotropic refinement was followed, after which all hydrogens attached to carbon were entered in ideal calculated positions and constrained to riding motion, with a single variable isotropic temperature factor for all of them. The two amino hydrogens were located in difference maps and allowed to refine independently. No unusually high correlations were noted between any of the variables in the last cycle of refinement, and the final difference map showed a maximum peak of about 0.5 e/Å^3. All calculations were made using Nicolet's SHELXTL PLUS (1987) series of crystallographic programs.

Table 1. Crystal Data Summary for $Sn(OCH(CF_3)_2)_4(HNMe_2)_2$

empirical formula	$C_{16}H_{18}N_2O_4F_{24}Sn$
f_w	877.05
crystal dim (mm)	0.30 × 0.35 × 0.45
space group	$P2_1/n$ (monoclinic)
a, Å	9.987(2)
b, Å	28.752(6)
c, Å	10.617(2)
β, deg	105.50(2)
temp, °C	−50
radiation (Mo Kα), Å	0.71073
Z	4
V, Å^3	2938
D_{calcd}, g/cm^3	1.98
μ, cm^{-1}	10.45
R, R_w[a]	0.028, 0.029

[a] $R = \sum||F_o| - |F_c||/\sum|F_o|$; $R_w = [\sum w(|F_o| - |F_c|)^2/\sum w|F_o|^2]^{1/2}$; $w = [\sigma(F)]^{-2}$.

Table 2. Atomic Coordinates (×10^4) for the Significant Atoms of $Sn(OCH(CF_3)_2)_4(HNMe_2)_2$

atom	*x*	*y*	*z*
Sn	5436(1)	1311(1)	2559(1)
O(1)	6444(3)	1700(1)	1534(2)
O(2)	6829(3)	1445(1)	4285(2)
O(3)	4404(3)	864(1)	3446(2)
O(4)	3921(3)	1200(1)	889(2)
N(1)	4231(3)	1898(1)	3113(4)
N(2)	6544(4)	683(1)	2097(4)
C(1)	5000(5)	2339(1)	3525(4)
C(2)	2826(4)	1999(2)	2293(5)
C(3)	7171(5)	372(1)	3197(5)
C(4)	7356(5)	714(2)	1141(5)
C(5)	7353(4)	2071(1)	1752(4)
C(6)	8834(5)	1913(2)	1950(5)
C(7)	6891(5)	2396(1)	582(4)
C(8)	7094(4)	1235(1)	5492(4)
C(9)	6355(5)	1483(2)	6388(4)
C(10)	8670(5)	1236(2)	6100(5)
C(11)	3081(4)	680(1)	2963(4)
C(12)	2235(5)	771(2)	3941(5)
C(13)	3172(5)	159(2)	2714(5)
C(14)	3868(4)	1258(1)	−409(3)
C(15)	2840(6)	1636(2)	−1023(5)
C(16)	3464(6)	793(2)	−1105(4)

Thin Film Depositions. General Procedures. Depositions were carried out in the UH Department of Chemistry using a cold-wall low pressure 1.75-in. tubular glass reactor (**I**). The inlet lines were 0.25-in. o.d. The substrate platform was a resistively heated aluminum block which was monitored

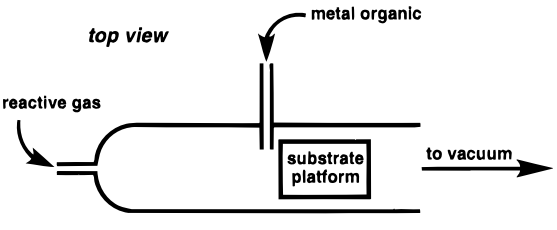

I

(21) Aboaf, J. A. *J. Electrochem. Soc.* **1967**, *114*, 948.
(22) Adachi, M.; Okuyama, K.; Tohge, N.; Shimada, M.; Sato, J.; Muroyama, M. *Jpn. J. Appl. Phys.* **1993**, *32*, L748.
(23) Battiston, G. A.; Gerbasi, R.; Porchia, M.; Marigo, A. *Thin Solid Films* **1994**, *239*, 186.
(24) Jeffries, P. M.; Girolami, G. S. *Chem. Mater.* **1989**, *1*, 8.
(25) Auld, J.; Houlton, D. J.; Jones, A. C.; Rushworth, S. A.; Malik, M. A.; O'Brian, P.; Critchlow, G. W. *J. Mater. Chem.* **1994**, *4*, 1249.
(26) Samuels, J. A.; Chiang, W.-C.; Yu, C.-P.; Apen, E.; Smith, D. C.; Baxter, D. V.; Caulton, K. G. *Chem. Mater.* **1994**, *6*, 1684.
(27) Jones, K.; Lappert, M. F. *J. Chem. Soc.* **1965**, 1944.
(28) Suh, S.; Hoffman, D. M. *Inorg. Chem.* **1996**, *35*, 6164.

with a thermocouple. The edge of the substrate was located approximately 12 in. from the reactive gas inlet and <0.5 in. from the metal−organic inlet. The base pressure for the system was (1.4−2.0) × 10^{-2} Torr. Helium and oxygen flow rates were controlled with mass flow controllers. When air was used as the reactive gas, it was admitted to the reactor via a Teflon bleed valve, and when oxygen (extra-dry grade) was used, it was diluted before entering the reactor with ultrahigh-purity helium (40 sccm O_2 in 160 sccm He).

Depositions from $Sn(OCH(CF_3)_2)_4(HNMe_2)_2$. Air was the reactant gas in this case. The precursor sublimator vessel and the precursor feed line were maintained at 110−120 °C with heating tape. The deposition pressure was 0.45−0.47 Torr. After the sublimator was shut off for a given run, the films were left under a flow of air for 3 min while maintaining the deposition temperature. The air bleed valve was then closed, and the films were slowly cooled under dynamic vacuum.

Depositions from $Sn(OCH(CF_3)_2)_2(HNMe_2)$. The precursor sublimator vessel and feed line were maintained at 90−100 °C with heating tape. The deposition pressure was 0.45−0.70 Torr for experiments using air as the oxide source. An ice-cooled flask containing degassed H_2O was connected to the CVD reactor when water was used as the oxide source. The deposition pressure was 0.10−0.15 Torr. In all experiments, after the sublimator was shut off for a given run, the films were left under a flow of air (via the Teflon bleed valve) for 3 min while maintaining the deposition temperature before being cooled under a flow of air.

Film Characterization. Backscattering spectrometry was used to determine film composition (Sn, C, N, O, and F) and thickness. In all cases the data were modeled and analyzed using the program RUMP. Infrared spectra were collected on a Mattson Galaxy 5000 FT-IR in the 400−4000 cm^{-1} range, and transmittance spectra were collected on a Hewlett-Packard 8452A diode array spectrophotometer.

For films deposited from $Sn(OCH(CF_3)_2)_4(HNMe_2)_2$, ion beam analyses were performed at the Texas Center for Superconductivity (NEC 2 × 1.7 MeV Pelletron tandem accelerator). Backscattering experiments were performed with a moderately high energy 3.48-MeV $^4He^{2+}$ beam,[29] which provided for enhanced sensitivity for the light elements relative to Sn. Data were typically acquired with a beam current of 20 nA until a charge of 4−10 μC was accumulated. Nuclear reaction analyses (NRA) for the detection of fluorine was performed using 1.25-MeV H^+. The reaction was $^{19}F(p,\alpha)^{16}O$. In the experiment, the detector was at an angle of 165° with respect to the incident beam, a Mylar foil was used to capture scattered protons, and a Teflon sheet was used as the standard. Resistivities were measured using the van der Pauw method[30] for films deposited on silicon (the substrate resistivity was 30 Ω cm). The films were heated to 250 °C to make the indium contacts for the measurements. The film thicknesses used in the calculations were obtained from the backscattering spectra.

For films deposited from $Sn(OCH(CF_3)_2)_2(HNMe_2)$, the ion beam (NEC 9SDH-2 Pelletron tandem accelerator) and Auger electron spectroscopy (AES, Physical Electronics 545) experiments were carried out at Los Alamos National Laboratory. A 2.0-MeV $^4He^+$ beam was used to collect the backscattering spectra. Data were typically acquired with a beam current of 30 nA until a charge of 9 μC was accumulated. Hydrogen content was measured by elastic recoil detection spectrometry (ERD) using a 2.0-MeV $^4He^+$ beam. A 10 μm Mylar foil was placed in front of the detector to absorb heavy ions, and Kapton ($C_{22}H_{10}N_2O_5$) foil was used as the standard. Auger electron spectroscopy depth profiling used a 3.5-keV Ar^+ sputter gun and was performed over a 2 × 2 mm^2 raster. The background pressure during depth profiling was 3 × 10^{-8} Torr, the electron beam energy was 3 keV, and the current was 200 nA. Sheet resistances were measured for films deposited on silicon by the four-point probe method and converted to local film resistivities by using film thicknesses obtained from backscattering spectra.

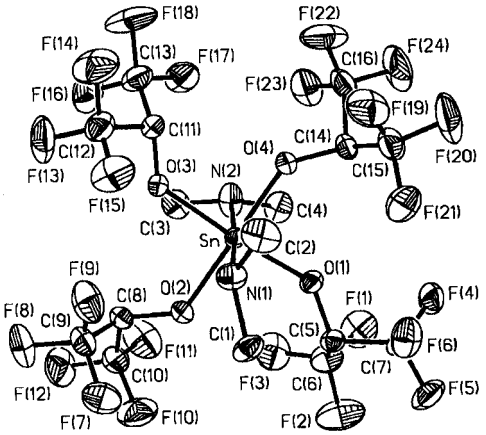

Figure 1. Thermal ellipsoid plot of $Sn(OCH(CF_3)_2)_4(HNMe_2)_2$ showing the atom numbering scheme (40% probability ellipsoids).

Table 3. Selected Bond Distances (Å) and Angles (deg) for $Sn(OCH(CF_3)_2)_4(HNMe_2)_2$

Sn−O(1)	2.009(3)	Sn−O(2)	2.019(2)
Sn−O(3)	2.029(3)	Sn−O(4)	2.025(2)
Sn−N(1)	2.241(4)	Sn−N(2)	2.239(4)
O(1)−Sn−O(2)	93.5(1)	O(1)−Sn−O(3)	173.9(1)
O(2)−Sn−O(3)	90.7(1)	O(1)−Sn−O(4)	88.8(1)
O(2)−Sn−O(4)	175.4(1)	O(3)−Sn−O(4)	87.3(1)
O(1)−Sn−N(1)	96.0(1)	O(2)−Sn−N(1)	84.6(1)
O(3)−Sn−N(1)	88.9(1)	O(4)−Sn−N(1)	91.2(1)
O(1)−Sn−N(2)	89.0(1)	O(2)−Sn−N(2)	95.3(1)
O(3)−Sn−N(2)	86.2(1)	O(4)−Sn−N(2)	88.8(1)
N(1)−Sn−N(2)	175.0(1)	Sn−O(1)−C(5)	138.0(2)
Sn−O(2)−C(8)	132.5(2)	Sn−O(3)−C(11)	128.4(2)
Sn−O(4)−C(14)	132.7(2)		

Results and Discussion

Synthesis and X-ray Structure of $Sn(OCH(CF_3)_2)_4(HNMe_2)_2$. $Sn(OCH(CF_3)_2)_4(HNMe_2)_2$, a moderately air-sensitive colorless solid, was synthesized in high yield by reacting $Sn(NMe_2)_4$ with $(CF_3)_2CHOH$ (eq 1). The complex can be purified by low-temperature crystallization or vacuum sublimation (70−75 °C at 0.06 Torr).

$$Sn(NMe_2)_4 + 4(CF_3)_2CHOH \rightarrow Sn(OCH(CF_3)_2)_4(HNMe_2)_2 + 2HNMe_2 \quad (1)$$

A thermal ellipsoid plot from the X-ray crystal structure determination of $Sn(OCH(CF_3)_2)_4(HNMe_2)_2$ is shown in Figure 1, and selected bond distances and angles are listed in Table 3. The molecule has octahedral coordination with virtual D_{4h} symmetry in the SnO_4N_2 core. The angles between the atoms in the core are all within 6° of 90°.

There are no significant differences in the four Sn−O or two Sn−N distances as judged by the 3σ criterion. The Sn−O distances (average 2.021(3) Å) are slightly longer than the bond lengths (1.923(7)−1.964(7) Å) reported for $Sn(O\text{-}t\text{-}Bu)_4$ and $[Sn(OR)_4(ROH)]_2$, R = *i*-Pr or *i*-Bu,[31,32] and the Sn−N distances (average 2.240(4)

(29) Zheng, Z. S.; Liu, J. R.; Cui, X. T.; Chu, W. K.; Rangarajan, S. P.;. Hoffman, D. M. *J. Mater. Res.* **1995**, *10*, 3124.
(30) Van der Pauw, L. J. *Philips Res. Rep.* **1958**, *13*, 1.
(31) Hampden-Smith, M. J.; Wark, T. A.; Rheingold, A.; Huffman, J. C. *Can. J. Chem.* **1991**, *69*, 121.
(32) Chandler, C. D.; Caruso, J.; Hampden-Smith, M. J.; Rheingold, A. L. *Polyhedron* **1995**, *14*, 2491.

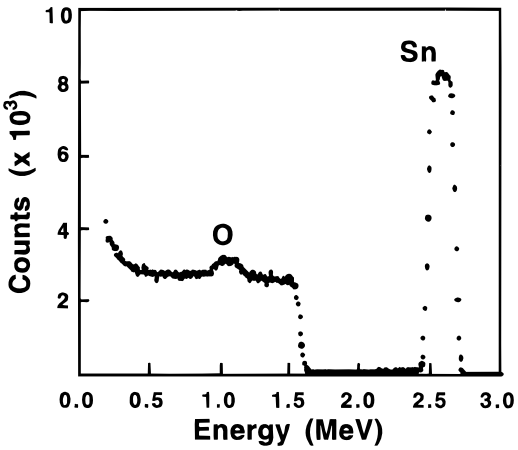

Figure 2. Backscattering spectrum for a tin oxide film deposited on silicon from $Sn(OCH(CF_3)_2)_4(HNMe_2)_2$ and air at 300 °C. Beam: 3.48-MeV $^4He^{2+}$.

Table 4. Composition of Tin Oxide Films Deposited on Silicon from $Sn(OCH(CF_3)_2)_4(HNMe_2)_2$ and Air

deposition temp (°C)	O/Sn[a]	F/Sn[b]
200	2.4	0.006
250	2.3	0.008
300	2.4	0.026
350	2.0	0.014
400	2.0	0.005
450	1.8	0.024

[a] From backscattering spectra. The error is estimated to be ±0.1. [b] From NRA. The error in the atomic ratio is estimated to be ±10%.

Å) are shorter than in $Sn(OC_6H_3PhC_6H_4)_2(HNMe_2)_2$ (2.32(1) Å).[33] The longer Sn−O and shorter Sn−N distances are probably due to the electron-withdrawing nature of the CF_3 groups, which reduces the alkoxide π donating ability and, in turn, allows the amine to be a more effective σ donor. More structural data are needed, however, to draw firm conclusions.

CVD Studies. Depositions from $Sn(OCH(CF_3)_2)_4(HNMe_2)_2$. Low-pressure CVD using $Sn(OCH(CF_3)_2)_4(HNMe_2)_2$ and air gave films at substrate temperatures of 200−450 °C. The films adhered well to the substrates when subjected to a tape test. Attempted depositions using $Sn(OCH(CF_3)_2)_4(HNMe_2)_2$ alone or in combination with dry O_2 did not give films in the same temperature range, suggesting that water vapor is the critical reactant. An X-ray diffraction pattern for a film deposited at 450 °C on glass indicated it was amorphous. It is not clear why our films are amorphous since previous reports on the growth of CVD tin oxide films at comparable temperatures indicate they are usually polycrystalline. In general, however, the crystallinity of tin oxide films is important for applications only in that the crystallinity affects surface roughness. Films with a rough surface are needed for amorphous silicon solar cells, and smooth films are needed for window and flat-panel display applications.[2,11,12]

Analyses of backscattering spectra (e.g., Figure 2) indicate the films have O/Sn ratios of 1.8−2.4 with the ratios decreasing as the temperature of deposition is increased (Table 4). Carbon, nitrogen, and fluorine peaks are not observed in the backscattering spectra, indicating low levels of these elements in the films (<3 atom %). The higher O/Sn ratios at deposition temperatures <350 °C are probably due to hydroxyl tin (≡SnOH) groups in the films resulting from incomplete reaction of intermediates (e.g., ≡Sn−OH + HO−Sn≡ → ≡Sn−O−Sn≡ + H_2O). Transmittance IR spectra show a very broad band around 3300 cm^{-1} that may be due to the O−H stretch.

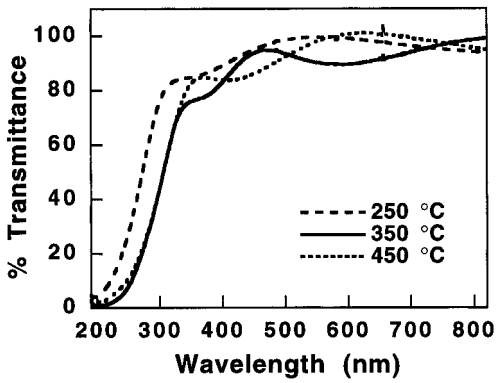

Figure 3. Transmittance spectra for tin oxide films deposited on quartz from $Sn(OCH(CF_3)_2)_4(HNMe_2)_2$ and air at 250, 350, and 450 °C.

NRA for fluorine gives F/Sn ratios of 0.005−0.026 with the amount of fluorine in the films varying randomly with deposition temperature. The fluorine content is comparable to the amount in films prepared from $Sn(O_2CCF_3)_2$ and O_2 (F/Sn ≈ 0.027).[14] The optimum amount of fluorine doping in tin oxide films has not been established because it will depend upon how effectively the incorporated fluorine contributes to the carrier concentration (i.e., the doping efficiency).[2] By using the fluorinated ligands as the fluorine source in our films, we have no control over the amount of flourine that is incorporated, which is a potential disadvantage of using this system.

Film thicknesses obtained from the backscattering spectra indicate growth rates are ≈1000 Å/min and that the rates are independent of the deposition temperature. In one case (300 °C) a rate of 2500 Å/min was observed, but the measurement was complicated by the fact that the film did not have a uniform thickness across the substrate at this temperature.

Selected transmission spectra for 4800−6000 Å thick films grown on quartz are shown in Figure 3. The absorption edge of the film deposited at 250 °C is shifted to higher energy compared to the films deposited at 350 and 450 °C. The films have >85% transmittance in the visible and near-IR regions, which is close to or higher than the transmittances reported for other CVD films; for example, Maruyama and Tabana reported transmittances of >80% for films grown at >250 °C from bis(trifluoroacetate)tin(II) and air.[14]

Optical bandgaps were calculated from the absorbance data by plotting α^2E^2 vs E and extrapolating the linear portion of the curve to $\alpha^2E^2 = 0$, where α is the absorption coefficient and E is the photon energy. At 250, 350, and 450 °C the bandgaps are 4.5, 4.1, and 4.1 eV, respectively, which are within the range of values reported for other SnO_2 and fluorine-doped SnO_2 films prepared by CVD (3.6−4.3 eV).[10,15,34]

(33) Smith, G. D.; Fanwick, P. E.; Rothwell, I. P. *J. Am. Chem. Soc.* **1989**, *111*, 750.

(34) Jarzebski, Z. M.; Marton, J. P. *J. Electrochem. Soc.* **1976**, *123*, 333C.

Table 5. Composition and Growth Rates of Films Deposited from $Sn(OCH(CF_3)_2)_2(HNMe_2)$ and Air or Water Vapor

deposition temp (°C)	composition[a]	growth rate (Å/min)
200[b]	$SnO_{1.0}F_{0.3}$	260
250[b]	$SnO_{0.9}F_{0.1}$	580
180[c]	$SnO_{1.1}F_{0.4}$	3900
200[c]	$SnO_{1.3}F_{0.3}$	4600
225[c]	$SnO_{1.2}F_{0.2}$	6200
250[c]	$SnO_{1.1}F_{0.1}$	7000

[a] Determined by backscattering spectrometry. The error is estimated to be ±0.1. [b] Deposition carried out with air as the reactant gas. [c] Deposition carried out with water vapor as the reactant gas.

Resistivities for the films deposited on silicon, which were measured by the van der Pauw method, ranged from 2×10^{-2} to 2×10^{-3} Ω cm with the lowest resistivities measured for the films grown at 400 and 450 °C. These values are higher than those reported ($(3-6) \times 10^{-4}$ Ω cm) for fluorine-doped SnO_2 films prepared by Gordon et al.[2] and Maruyama and Tabata.[14]

Depositions from $Sn(OCH(CF_3)_2)_2(HNMe_2)$. $Sn(OCH(CF_3)_2)_2(HNMe_2)$ (**II**) is a volatile (subl. 50−55 °C/0.1 Torr) solid that was prepared readily from $Sn(NMe_2)_2$ and $(CF_3)_2CHOH$ in high yield.[28] Low-pressure

II

chemical vapor deposition using $Sn(OCH(CF_3)_2)_2(HNMe_2)$ and air or deionized water vapor as precursors gave films at substrate temperatures of 180−450 °C. The as-deposited films grown at ≤250 °C were shiny, but those grown at higher temperatures had a "milky" appearance. Also, films deposited at <200 °C using water vapor developed whitish blotches over a period of months. All of the films adhered well to the substrates (silicon, glass, and quartz), but when films deposited at ≤250 °C were annealed for 1 h at ≥250 °C, they peeled from the substrate. Attempted depositions using $Sn(OCH(CF_3)_2)_2(HNMe_2)$ alone or in combination with dry O_2 did not give films at substrate temperatures of 250−450 °C, suggesting that water is the critical reactant in the deposition process.

Analyses of backscattering spectra indicate the films grown using air or water as co-reactant have similar compositions with O/Sn = 0.9−1.3 and F/Sn = 0.1−0.4 (Table 5). Films deposited at 200 °C using air or water have <10 atom % H incorporation as determined by ERD. The fluorine content of the films decreased as the deposition temperature was increased for both precursor mixtures. Carbon peaks are not observed in the backscattering spectra, suggesting <5 atom % contamination. Consistent with this, an AES analysis for the film deposited at 200 °C on silicon using water vapor as the co-reactant showed no carbon peaks after sputtering into the bulk. Film growth rates were dramatically higher using water vapor as the oxygen source, and the growth rates increased as the temperature of deposition increased.

Transmittance spectra for four films deposited on quartz are shown in Figure 5. The films deposited at

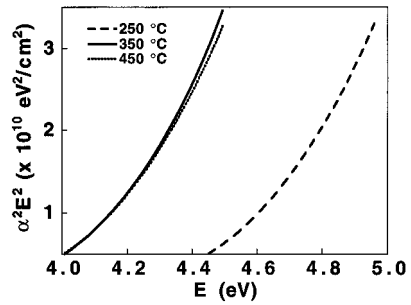

Figure 4. Plots to determine bandgaps for tin oxide films deposited on quartz from $Sn(OCH(CF_3)_2)_4(HNMe_2)_2$ and air at 250, 350, and 450 °C.

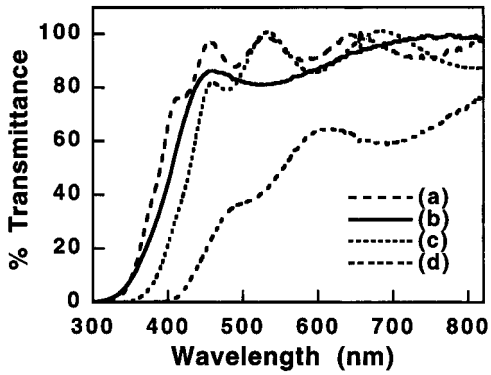

Figure 5. Transmittance spectra for tin oxide films deposited on quartz from $Sn(OCH(CF_3)_2)_2(HNMe_2)$ and (a) water vapor at 200 °C, (b) water vapor at 250 °C, (c) air at 250 °C, and (d) air at 400 °C.

or below 250 °C show good transparency in the visible. Films deposited at higher temperatures or those that were annealed at ≥250 °C for 30 min or more in the presence or absence of O_2 are much less transparent. Bandgaps, which were determined using the absorbance data, are 3.0−3.3 eV for films deposited at 200−250 °C. Four-point probe measurements for the films deposited at ≤250 °C using water as co-reactant indicate they are not conductive with the exception of the one deposited at 250 °C, which had a resistivity of 0.027 Ω cm.

The film stoichiometries and properties suggest that $Sn(OCH(CF_3)_2)_2(HNMe_2)$ was not oxidized by O_2 during deposition. This contrasts sharply with the results obtained in other CVD studies where tin(II) precursors were used. Maruyama and Ikuta, for example, found that $Sn(acac)_2$ and air gave SnO_2 films but that $Sn(acac)_2$ and water vapor gave SnO films via hydrolysis.[16] Also, $Sn(O_2CCF_3)_2$ and air gave fluorine-doped SnO_2 films.[14] Similar results were obtained in a spray pyrolysis study that used $SnCl_2$ as the tin precursor. The suggested mechanism involved initial formation of SnO via hydrolysis followed by O_2 oxidation to SnO_2 at temperatures >250−300 °C.[35] On the basis of this proposal, the milky appearance of the films we deposited at >250 °C may be due to surface oxidation of SnO to SnO_2. Also, the loss of transparency and delamination that occurs upon heat treatment of our SnO films may be due to decomposition of SnO to tin and SnO_2, as observed for films deposited at >200 °C by dc reactive sputtering.[5]

(35) Gordillo, G.; Moreno, L. C.; de la Cruz, W.; Teheran, P. *Thin Solid Films* **1994**, *252*, 61.

Conclusion

Low-pressure chemical vapor deposition using $Sn(OCH(CF_3)_2)_4(HNMe_2)_2$ and air gave fluorine-doped tin oxide films (O/Sn = 1.8−2.4) at substrate temperatures of 180−450 °C. The films were highly transparent in the visible region (>85%) and electrically conductive. A film deposited at 450 °C with a F/Sn ratio of 0.024 had the lowest resistivity (2.1×10^{-3} Ω cm). This value is a factor of 5 higher than the lowest resistivities reported for CVD films.[2,14]

Films prepared from $Sn(OCH(CF_3)_2)_2(HNMe_2)$ and air or water vapor were different from those obtained using the tin(IV) precursor. At substrate temperatures of 200−250 °C, nonconductive transparent films were deposited having composition $SnO_{0.9-1.3}F_{0.1-0.4}$. The film stoichiometries and properties suggest that the tin(II) precursor was not oxidized during the deposition and that hydrolysis was the primary film forming reaction.

Acknowledgment for support is made to the Environmental Institute of Houston, Los Alamos National Laboratory, the State of Texas through the Texas Center for Superconductivity at the University of Houston, and the Robert A. Welch Foundation. We thank Dr. James Korp for his technical assistance with the crystal structure determination and his helpful discussions.

Supporting Information Available: Tables of data and processing parameters, atomic coordinates, thermal parameters, bond distances and angles, and packing diagram for $Sn(OCH(CF_3)_2)_4(HNMe_2)_2$ (8 pages); observed and calculated structure factors (19 pages). Ordering information is given on any masthead page.

CM960423T